Engineering Fracture Mechanics 192 (2018) 343–361

Contents lists available at ScienceDirect

Engineering Fracture Mechanics

journal homepage: www.elsevier.com/locate/engfracmech

Fracture analysis of the set-in nozzle of a PWR reactor pressure vessel – Part 1: Determination of critical crack

Usman Tariq Murtaza *, M. Javed Hyder

Department of Mechanical Engineering, Pakistan Institute of Engineering and Applied Sciences, Islamabad 45650, Pakistan

ARTICLE INFO

Article history:
Received 12 November 2015
Received in revised form 13 March 2016
Accepted 23 March 2016
Available online 7 June 2016

Keywords:
Set-in nozzle
RPV
SB-LOCA
RST

ABSTRACT

In this study, fracture mechanics analysis of the set-in nozzle of a reactor pressure vessel (RPV) is being presented. The selected RPV belongs to a 300 MW pressurized water reactor (PWR). For the purpose, a wide range of elliptical surface cracks was analyzed at the nozzle-cylinder intersection under two accidental conditions of the reactor: small-break loss of coolant accident (SB-LOCA), and Rancho-Seco transient (RST). It has been demonstrated that at the location being investigated '$a = 0.05t$' is the critical crack depth; where 'a' is the depth/minor axis of the crack and 't' is the thickness of the wall.

1. Introduction

The reactor pressure vessels (RPV), during their service, have to operate under normal operating and accidental conditions of the plant. The fracture mechanics analysis of different parts of the RPV under normal operating conditions [1–3] is quite straight forward; however the analysis becomes critical under accidental conditions of the plant. In this paper, the fracture analysis of the set-in nozzle of an RPV is being presented under accidental conditions of the plant [4]. The considered RPV is made of nuclear grade steel *'SA-508 Gr.3 Cl.1'* [5] and it belongs to a 300 Megawatts (MW) pressurized water reactor (PWR) [4].

The accidental conditions taken for the analysis are the small break loss of coolant accidental conditions (SB-LOCA), and the Rancho-Seco transient (RST) conditions of the PWR. For the fracture analysis the highest stress concentration point (HSCP) of the nozzle, under normal operating conditions of the plant [1,4] is selected: the nozzle-cylinder intersection. A wide range of corner surface cracks has been analyzed at the nozzle-cylinder intersection under the accidental conditions. The limits of the cracks were '$0.01 < a/t < 0.25$' with '$a = 0.33c$', where 'a' and 'c' represent minor and major axis of the crack respectively; and 't' is the thickness of the vessel's wall at the nozzle-cylinder intersection. The stress intensity factors (SIFs) of all the cracks under the accidental conditions were evaluated using the 'pallet body approach' of the crack modeling [6–8]. It is a finite element methods (FEM) based computational technique for crack analysis.

1.1. Goal of the research

The goal of this study was to investigate the critical crack depth at the nozzle-cylinder intersection of the RPV under the accidental conditions of the plant. For the purpose, the SIFs of a wide range of corner cracks were compared with the fracture

* Corresponding author.
E-mail addresses: maniiut@yahoo.com (U.T. Murtaza), hyder@pieas.edu.pk (M. Javed Hyder).

http://dx.doi.org/10.1016/j.engfracmech.2016.03.049
0013-7944/

Nomenclature

a	depth or minor axis of the elliptical corner surface crack
c	major axis of the elliptical corner surface crack
f	neutron fluence
t	thickness of the RPV wall at the set-in nozzle intersection
E	Young's modulus of material
α	angle between set-in nozzle and set-out nozzle
ϕ	angle of the crack tip with major axis of the crack
v	Poission's ratio
E_{neu}	neutron energy
K_{IC}	fracture toughness of a material
K_{JN}^{ps}	EPFM based SIF under both pressure (primary) & thermal (secondary) loadings in normal operating conditions
K_{IS}^{ps}	LEFM based SIF under both pressure (primary) & thermal (secondary) loadings in SB-LOCA accidental conditions
K_{JS}^{ps}	EPFM based SIF under both pressure (primary) & thermal (secondary) loadings in SB-LOCA accidental conditions
K_{IR}^{ps}	LEFM based SIF under both pressure (primary) & thermal (secondary) loadings in RST accidental conditions
K_{JR}^{ps}	EPFM based SIF under both pressure (primary) & thermal (secondary) loadings in RST accidental conditions
σ_h	hoop stress
PWR	pressurized water reactor
RPV	reactor pressure vessel
SB-LOCA	short break loss of coolant accident
RST	Rancho-Seco transient
ICS	integrated control system
EOL	end of life
HSCP	highest stress concentration point
SIF	stress intensity factor
LEFM	linear elastic fracture mechanics
EPFM	elastic plastic fracture mechanics
FF	fluence factor
CF	chemistry factor

toughness value of the RPV's steel (*SA-508 Gr.3 Cl.1*). The effects of the material's embrittlement due to the nuclear environment have also been incorporated in the fracture toughness of the material.

1.2. Literature review

Fracture mechanics analyses or safety analyses of RPVs under various loading conditions have been an active area of research for the last few decades. In this context, Bangash [9] in 1984, performed a finite element based analysis and design of Sizewell-B type RPV under normal and unanticipated events of the plant. He demonstrated that the most important areas of the RPV from the fracture assessment point of view are inlet and outlet nozzles, top and bottom head, and the beltline region of the vessel. He plotted hoop stress distributions under pressure loading of 17.24 MPa for different regions of the RPV and corroborated the results for inlet and outlet nozzles.

In 1999, Siegele et al. [10], performed fracture mechanics analysis of the RPV's nozzle under loss of coolant accident (LOCA). In the study, they have presented that the nozzle regions face higher stresses and lower temperature in the event of the LOCA, and is therefore vulnerable and may threaten the integrity of the RPV. Hence, the safety assessment of the nozzle must be performed. After postulating the circular cracks at nozzle-cylinder intersection, they computed SIFs as functions of crack tip temperatures. In their study, the analytical approaches used for solutions of surface cracks in cylindrical portions were extended for the solutions of corner cracks at the nozzle-cylinder intersection. In the same year, Kim and Jin [11], performed structural integrity analysis of an RPV under the external reactor vessel cooling condition. The integrity analysis of the lower head of the RPV was performed during the transient state of reactor vessel cooling.

In 2000, He and Isozaki [12], performed fracture mechanics analysis of the beltline region of the RPV of a Chinese pressurized water reactor. The authors conducted the fracture analysis under small-break loss of coolant accident, large-break loss of coolant accident and Rancho-Seco transients. They employed ADINA code for development of crack mesh and for the fracture analysis. They investigated that which type of flaw and transient condition is most detrimental for the beltline region of the RPV. They also demonstrated that large-break loss of coolant accident is less severe pressurized thermal shock when compared to small-break loss of coolant accident and Rancho-Seco transients. The authors assessed the fracture integrity of the RPV by comparing the stress intensity factors of different cracks with the fracture toughness of the material.

In 2001, Colak and Ozdere [13] performed a comparative study of a four loop reactor pressure vessel's integrity under different LOCA conditions. Deterministic and probabilistic approaches were employed for the analysis of beltline region under pressurized thermal shocks due to LOCA conditions. Computer code VISA-II was utilized for the calculations of vessel's failure probabilities. Among the analyzed cases, a medium break loss of coolant accident induced by a 50-cm^2 break in the hot leg yields the higher vessel rupture probability. In 2003, Colak and Ozdere [14] also conducted the integrity analyzes of reactor pressure vessels of eastern and western pressurized water reactors.

In 2014, Chen et al. [15], performed fracture mechanics analysis of the beltline region of a reactor pressure vessel under the event of pressurized thermal shock. The authors stated that analysis under such unanticipated events is the key element of the integrity evaluation. They computed SIFs of five semi-elliptical surface cracks postulated in the beltline region of RPV in order to investigate the most detrimental crack. They accomplished the fracture evaluation by comparing the SIFs of the cracks with the fracture toughness of the used material. They concluded that while analyzing the surface cracks in the RPV, both the deepest and surface (edge) point of the crack should be considered because the safety margin at the deepest point is not always smaller than that of the surface point.

In 2015, Murtaza and Hyder [6] performed fracture mechanics analysis of the set-in nozzle under normal operating conditions of the plant. They have also incorporated the effects of operational thermal stresses on the SIFs of the corner cracks. They concluded that the set-in nozzle is a safe design and even the worst corner crack [16] does not threaten the integrity of the nozzle under normal operating conditions.

1.3. Need of the research

Based on the literature review, it has been observed that the fracture mechanics analysis covering the behaviour of corner cracks at the nozzle-cylinder intersection especially under SB-LOCA and RST conditions is missing in the contemporary literature. Hence, a research work was required, which presents the SIFs for a wide range of corner cracks (starting from a minute crack) under the conditions. Here in this paper, both linear elastic fracture mechanics (LEFM) and elasto-plastic fracture mechanics (EPFM) based SIFs of the corner cracks are presented in a suitable graphical format, which provides a useful tool for the fracture analysis of the nozzle. With the help of these SIFs, the critical crack depth at the nozzle-cylinder intersection is successfully investigated in this research work. However, the simulations of the fatigue crack growth up to the critical depth will be presented soon as the second part of this research work. The second part will also include computations of the safe life of the RPV in the presence of manufacturing defect at the nozzle-cylinder intersection.

2. Problem description

2.1. The reactor pressure vessel and the set-in nozzle

The engineering drawing of a typical double loop cylindrical RPV [1,3] of a 300 MW pressurized water reactor is shown in Fig. 1. Fig. 1(a) shows the cut-section view of the vessel through the inlet and outlet nozzles. The vessel has two inlet and two outlet nozzles. Fig. 1(b) shows the top view of the reactor pressure vessel. The angle between the inlet and outlet nozzles is equal to 60° as shown by 'α' in Fig. 1(b). The vessel has a geometrical symmetry, and the plane of symmetry is as shown in

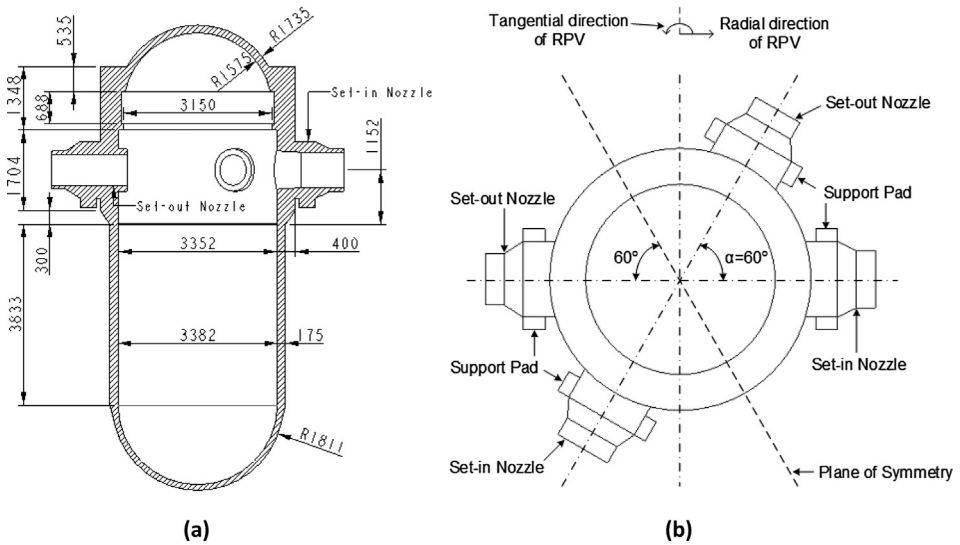

Fig. 1. Engineering drawing of the typical RPV [1,4] (a) cut-section view, dimensions in mm and (b) top view.

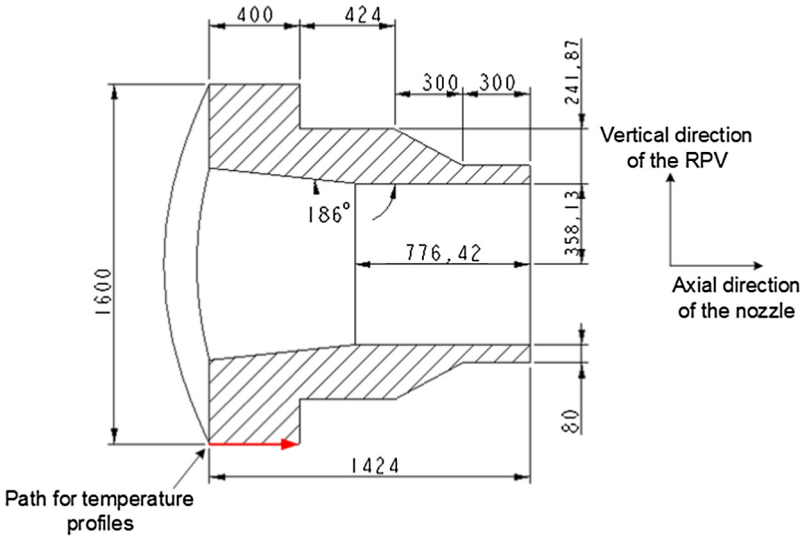

Fig. 2. The design of the typical set-in nozzle [1,4], dimensions in mm.

Fig. 1(b). The RPV is supported by providing the support pads under the inlet and outlet nozzles as shown in Fig. 1(b). Fig. 1 (b) also shows tangential and radial directions of the RPV.

The inlet nozzles usually used in such RPVs are the set-in nozzles, which have flange set into the vessel wall [3]. Fig. 2 presents the typical design of the set-in nozzle [1,4]. The thickness of the vessel's wall at the nozzle-cylinder intersection is denoted by parameter '*t*' which has the value '*t* = 400 mm' as shown in Fig. 2. The figure also shows vertical direction of the RPV, axial direction of the set-in nozzle, and path for temperature profiles (which will be used later in fracture mechanics analysis).

2.2. Material of the RPV

A nuclear grade steel, designated in ASME code as *'SA-508 Gr.3 Cl.1'* was selected as the material for the RPV [5]. The material has nominal composition as 3/4*Ni*-1/2*Mo*-*Cr*-*V*. The mechanical and thermal characteristics of the material are listed in Table 1 while the density of the material is 7750 kg/m^3 [5].

The true stress-strain characteristics of the material (*SA-508 Gr.3 Cl.1*) at room and at high temperatures are shown graphically in Fig. 3 [12].

2.2.1. The embrittlement of the material

It is a well-known fact that the nuclear environment, which is the environment of the RPV, causes embrittlement (loss of ductility) of the material. The fission chain reactions of U-235, in the core of the RPV, emit high-energy neutrons that affect the internal surface of the RPV. These neutrons (during collisions with the material) alter the behaviour of the material on the micro and nano-structural level; and hence, modify the mechanical properties of the material. One of these modifications is the embrittlement of the material. In fact, the embrittlement reduces the fracture toughness (K_{IC}) of the material by shifting the nil ductility transition point to the higher temperature [17].

Table 1
Mechanical and thermal characteristics of *'SA-508 Gr.3 Cl.1'* steel.

Temperature (°C)	Young's modulus (GPa)	Poisson's ratio	Yield strength (MPa)	Conductivity (W (m °C)$^{-1}$)	Specific heat (J/kg °C)	Mean coefficient of thermal expansion (1/°C)
50	191	0.3	345	38.3	465.81	1.18E−05
100	187	0.3	323	38.8	489.03	1.21E−05
150	184	0.3	314	38.8	508.39	1.24E−05
200	181	0.3	305	38.6	527.74	1.27E−05
250	178	0.3	299	38.1	545.81	1.30E−05
275	176	0.3	296	37.8	556.78	1.33E−05
288	175	0.3	294	37.6	562.26	1.35E−05
300	174	0.3	292	37.5	567.74	1.36E−05
350	171	0.3	285	36.8	588.39	1.36E−05

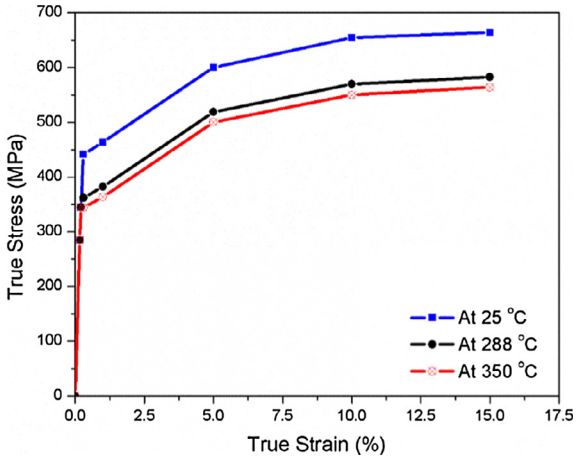

Fig. 3. True stress-strain characteristics of the *'SA-508 Gr.3 Cl.1'* steel [12].

In practice, neutrons having kinetic energy higher than '1 Mega electron-volt (MeV)' form the fluence that is considered to be capable of triggering damage mechanisms (embrittlement) in steels; these neutrons are referred to as fast neutrons. Typical design end-of-life (EOL) neutron fluence (E_{neu} > 1 MeV) for PWRs is in the order of around 10^{19} n/cm^2. According to '10 CFR 50.61' guide [18], fracture mechanics analysis of nuclear components should be performed considering the EOL neutron fluence, before the reactor is put into service. The US regulatory guide 'US R.G. 1.99' [19] contains an approach to calculate the fracture toughness of the material which incorporates the EOL neutron fluence. This regulatory approach has been used here in order to compute the fracture toughness value of *'SA-508 Gr.3 Cl.1'* steel.

2.2.2. The fracture toughness of the RPV's material

It is widely accepted that the average number of neutrons produced per fission reaction is about two and a half [20]. The majority of these neutrons are prompt neutrons emitted at the time of fission. A small fraction is of delayed neutrons, which typically appears from seconds to minutes later. The number of neutrons from fission depends upon both the identity of the fissionable nuclide and the energy of the incident neutron. The energy distribution or spectrum for neutrons emitted by fission is relatively independent of the energy of the neutron causing the fission. For many practical purposes, the empirical expression given in Eq. (1), provides an adequate approximation to the neutron spectrum during the fission of uranium-235 which happens in the core of the RPV [4,20].

$$n(E_{neu}) = 0.453e^{-1.036E_{neu}} \cdot \sinh(2.29E_{neu})^{0.5} \tag{1}$$

where E_{neu} is the energy of the neutron given in MeV. The neutron energy distribution (spectrum) has been plotted in Fig. 4, which indicates that the neutrons, produced in a nuclear fission reaction, have an energy ranging from 0.1 MeV to approx-

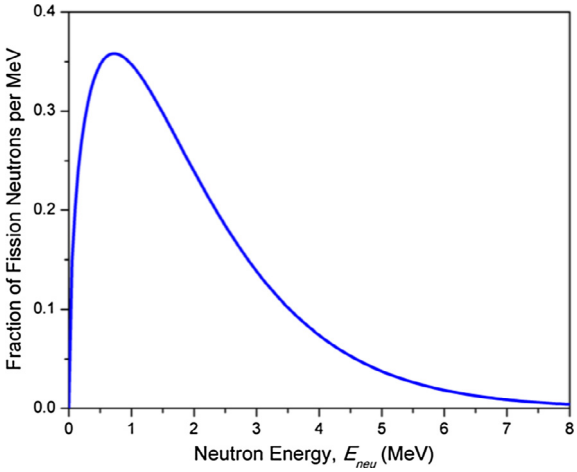

Fig. 4. Neutrons energy spectrum for thermal fission of U-235.

imately 8 MeV, and therefore they are called high-energy neutrons. The peak of the curve corresponds to the most probable fission neutron energy that is 0.7 MeV. However, the average energy of the neutrons produced in a fission reaction is 2 MeV; and hence they form a fluence that is capable of damaging the microstructure of the steel.

An analytical expression, given in ASME code [21], has been used for the determination of lower bound fracture toughness of the RPV's steel (*SA-508 Gr.3 Cl.1*) considering the effects of neutrons (neutron fluence). The analytical expression is called ASME reference critical stress intensity factor curve and is given by Eq. (2) [21].

$$K_{IC} = 36.5 + 22.783 \exp[0.036(T - RT_{NDT})] \tag{2}$$

where

K_{IC} = Fracture toughness of the material, in MPa$\sqrt{\text{m}}$.
T = Temperature, in °C.
RT_{NDT} = Nil-ductility transition reference temperature for irradiated material.

The 'RT_{NDT}' can be evaluated using Eq. (3) as given in US regulatory guide 'US R.G. 1.99' [19].

$$RT_{NDT} = \text{initial } RT_{NDT} + \Delta RT_{NDT} + \text{margin} \tag{3}$$

where

initial RT_{NDT} = Initial reference nil-ductility temperature of fresh material.
ΔRT_{NDT} = Increase in temperature as a result of irradiation.
margin = Account for uncertainties in the parameters.

The 'ΔRT_{NDT}' can be evaluated using Eq. (4) as given in the US regulatory guide 'US R.G. 1.99' [19].

$$\Delta RT_{NDT} = (\text{CF}) f^{(0.28 - 0.1 \log f)} = (\text{CF}) \times (\text{FF}) \tag{4}$$

where

f = Neutron fluence in units of 10^{19} n/cm^2 (E_{neu} > 1 MeV).
FF = Fluence factor.
CF = Chemistry factor based on the copper and nickel content.

In this study, a typical end-of-life fluence equal to 4×10^{19} n/cm^2 has been taken at the set-in nozzle of the RPV. The initial reference nil-ductility temperature was measured by drop weight and Charpy impact test of the material *'SA-508 Gr.3 Cl.1'* which is equal to −20°C and hence 'initial $RT_{NDT} = -20$ °C' [12]. Using the regulatory approach described above, the nil-ductility transition temperature for irradiated *'SA-508 Gr.3 Cl.1'* steel has been calculated which is 'RT_{NDT} = 79.6 °C'. Using this value, the Eq. (2) becomes as below.

$$K_{IC} = 36.5 + 22.783 \exp[0.036(T - 79.6)] \tag{5}$$

The ASME code, IWB-3613 [22] recommends that a safety factor of $\sqrt{2}$ should be applied on the fracture toughness value for the determination of critical crack dimensions at nozzle-cylinder intersection of the vessel. Using the factor of safety Eq. (5) becomes as below.

$$K_{IC} = 25.81 + 16.11 \exp[0.036(T - 79.6)] \tag{6}$$

The Eq. (6) gives lower bound fracture toughness value for *'SA-508 Gr.3 Cl.1'* steel. Using this exponential curve the fracture toughness increases without bound and this curve does not predict the upper bound fracture toughness. In ASME fitness-for-service standard [23,24], a cut-off to the exponential curve at $K_{IC} = 220$ MPa$\sqrt{\text{m}}$ is recommended for *'SA-508 Gr.3 Cl.1'* steel. Applying factor of safety equal to $\sqrt{2}$, the upper bound fracture toughness becomes $K_{IC} = 155.6$ MPa$\sqrt{\text{m}}$. The fracture toughness curve plotted using Eq. (6) and the upper bound fracture toughness value is given in Fig. 5.

This fracture toughness curve will be used as the limiting criteria for the determination of critical crack size under different operating conditions of the reactor.

2.3. Boundary conditions

The following boundary conditions (B.Cs) were applied for the fracture mechanics analysis of the set-in nozzle.

(1) Taking the advantage of the geometric and loading symmetry, as shown in Fig. 1(b), only half of the RPV was modeled for the analysis. The half of the RPV contains one set-in nozzle and one set-out nozzle.
(2) The mass of the full RPV, with the material *'SA-508 Gr.3 Cl.1'* is 193,280 kg. The effects of the weight of the RPV on the vessel's supports have also been considered in the analysis.

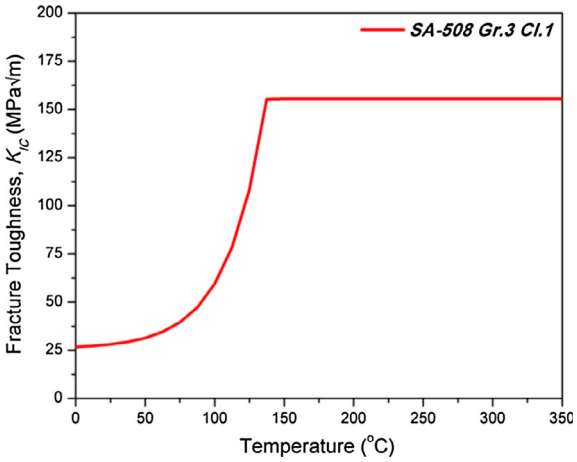

Fig. 5. Fracture toughness curve of irradiated *'SA-508 Gr.3 Cl.1'*.

(3) The support pads are constraint in tangential and radial directions of the RPV (see Fig. 1(b)) as well as in vertical direction of the RPV (see Fig. 2).
(4) Along with the support pads, in order to properly support the heavy vessel, the skirt type support is also recommended at the lower hemisphere of the vessel [25]. The lower hemisphere of the RPV was fixed in the analysis in order to incorporate the effects of skirt support. The assumption is valid in our case because the skirt support has negligible effects on the nozzle, which is very far away from the lower head of the RPV.
(5) The bending loads caused by the support pads on the nozzle have been taken into account.
(6) The effects of axial loads on the nozzle have also been considered. The effects are negligible [4] because the support pads are free to move in the axial direction of the nozzle.

2.4. Limitation of the research work

The following limitations may be taken into account whenever to refer this research work.

(1) The effects of cladding layer [4] on the behaviour of the cracks have been ignored throughout this research work.
(2) The effects of temperature changes along the height or vertical direction of the RPV (see Fig. 1) have been ignored.
(3) A constant neutron fluence has been used in this research work. However, in actual a negligible change in the fluence along the thickness of the vessel is observed.

2.5. Accidental conditions for the fracture mechanics analysis

The initial conditions, internal pressure of the RPV, and the temperature gradients in the vessel's wall were derived from the following SB-LOCA and RST conditions.

2.5.1. Small break loss of coolant accident

Small break loss of coolant accident (SB-LOCA) is one of the most severe accidental conditions of the pressurized water reactor. In SB-LOCA, cold safety water is injected into the RPV through the set-in nozzles, while the internal pressure remains at high level. This sudden cooling causes huge thermal (secondary) stresses, in addition to pressure (primary) stresses, in reactor pressure vessel. During this event, the highest thermal stresses are expected to be occurred at the set-in nozzle since the cold water is injected through this nozzle.

The event of SB-LOCA is called pressurized thermal shock (PTS) according to the 10 CFR 50.61 definition [18]. The fracture mechanics analysis under PTS transients is indispensable because such events result in much higher stresses as compared to normal operating conditions of the plant and may threaten the integrity of the RPV. In such events, relatively smaller cracks may become critical and may cause fracture of the structure. The fracture analysis under PTS requires a couple field structural-thermal analysis in which the combined effects of pressure plus thermal stresses should be considered. The temperature and pressure of the reactor's coolant under SB-LOCA conditions [12] are given in Fig. 6. The figure shows that at full power operation of the reactor SB-LOCA event continues for 5000 sec.

2.5.2. Rancho-Seco transient

The second accidental condition analyzed in this research work, is the Rancho-Seco transient (RST). Rancho-Seco nuclear power plant is a single unit, two-loop (Babcock and Wilcox) pressurized water reactor situated in USA. On December 26,

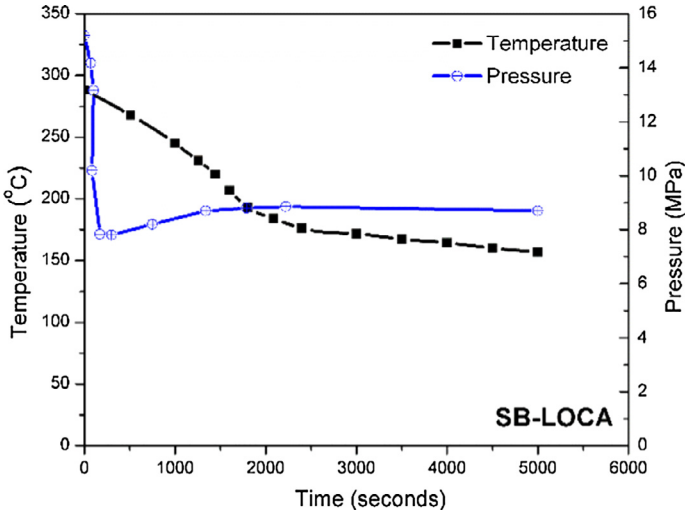

Fig. 6. Temperature and pressure of the coolant under SB-LOCA conditions.

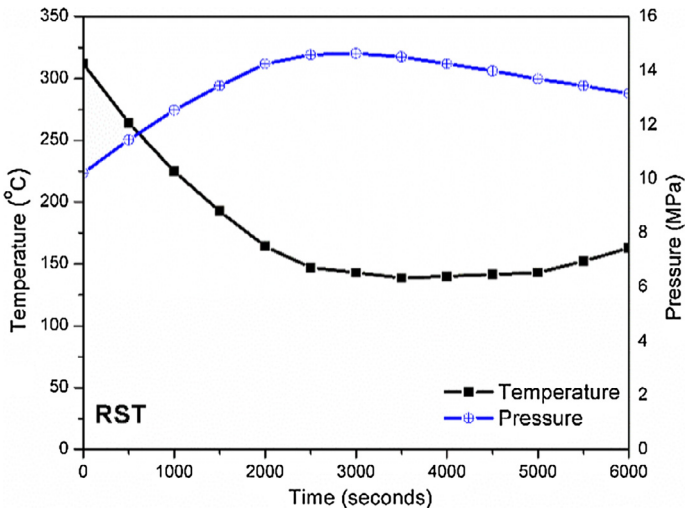

Fig. 7. Temperature and pressure of the coolant under RST.

1985 [26], power to the integrated control system (ICS) of the Rancho-Seco's reactor was lost during the operation. ICS demand signals automatically went to mid-scale, closing the main feed water valves to 50 percent and opening the atmospheric dump valves, turbine bypass valves, and one set of auxiliary feed water valves to 50 percent. The high pressure of the reactor coolant system, in turn, tripped off the reactor. It took the operators 26 min to restore power to the ICS (by flipping a switch from "off" to "on"). During the event, a severe PTS was observed because the temperature of the coolant of the reactor was dropped quickly while the internal pressure of the vessel was remained at higher level. Rancho-Seco transient as nuclear engineers call this event, is one of the most severe accidental conditions of the PWRs. The temperature and pressure of the reactor's coolant under RST conditions [12] are shown in Fig. 7. The figure shows that the RST event continues for 6000 sec.

2.6. Temperature profiles through the nozzle-belt

The temperature profiles through-the-thickness of the nozzle-belt along 'the path for temperature profiles' (see Fig. 2) were computed by performing the transient thermal analysis of the RPV. The initial conditions of SB-LOCA and RST incidents as given in Section 2.5 have been used for the transient thermal analysis. The temperature profiles under both the incidents at different time steps are given below.

2.6.1. Under SB-LOCA conditions

The SB-LOCA accidental conditions generate a pressurized thermal shock (PTS) that remains for 5000 sec as shown in Fig. 6. This duration was discretized into five steps of 1000 sec each for the computations of the temperature profiles. The computed temperature profiles at the time intervals of 1000 sec, 2000 sec, 3000 sec, 4000 sec, and 5000 sec are presented in Fig. 8.

2.6.2. Under RST conditions

The RST accidental conditions of the PWR generate a PTS that remains for 6000 sec as shown in Fig. 7. The event duration was divided into six steps in this case, and the temperature profiles at time intervals of 1000 sec, 2000 sec, 3000 sec, 4000 sec, 5000 sec, and 6000 sec are shown in Fig. 9.

The temperature differences, under SB-LOCA and RST conditions, between outer and inner surfaces of the nozzle-belt's wall are clear from Figs. 8 and 9, respectively. These temperature gradients will generate thermal stresses in the wall of the RPV in addition to the pressure stresses. The combined stresses (pressure plus thermal stresses) have been used for capturing the effects under pressurized thermal shocks during the SB-LOCA and the RST conditions.

3. The fracture mechanics analysis of the set-in nozzle

The fracture mechanics analysis of a component can generally be performed by postulating an initial crack of a defined size, which represents a crack size that is observed during non-destructive testing or which can be expected during the lifetime of the component [16]. For the fracture analysis of the set-in nozzle, the integrity confirmation at the nozzle-cylinder intersection is compulsory because it is the highest stress concentration point of the nozzle under normal operating

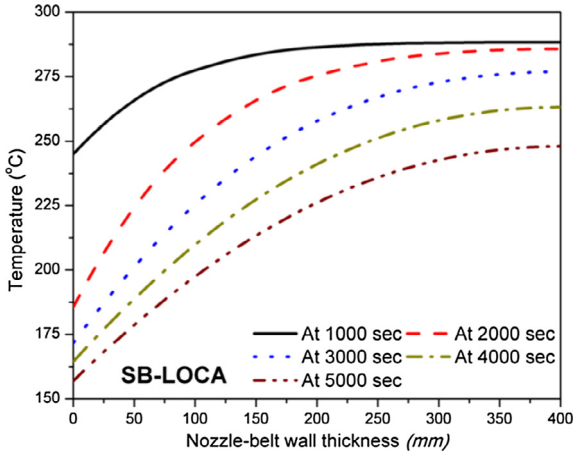

Fig. 8. Temperatures profiles through-the-thickness of the nozzle-belt under SB-LOCA conditions.

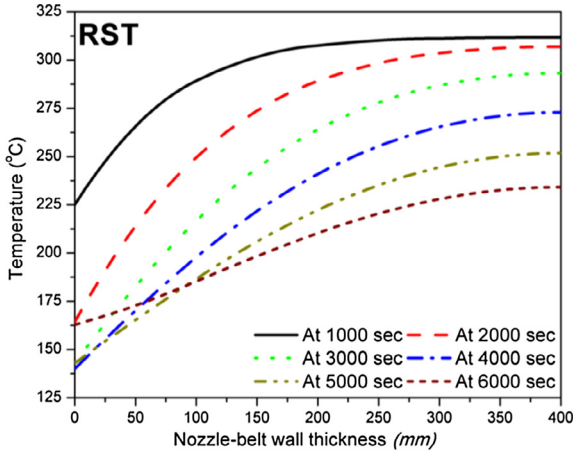

Fig. 9. Temperatures profiles through-the-thickness of the nozzle-belt under RST conditions.

conditions [6]. For the fracture analysis of the nozzle a wide range of corner cracks was postulated at the nozzle-cylinder intersection. The SIFs of all the corner cracks have been computed numerically under the SB-LOCA and the RST conditions. Both the linear elastic and elastic plastic material models were used in order to compute linear elastic fracture mechanics (LEFM) and elasto-plastic fracture mechanics (EPFM) based SIFs of the corner cracks. These SIFs have been finally compared with the fracture toughness value of the RPV's steel (*SA-508 Gr.3 Cl.1*), in order to determine critical depth of the crack.

3.1. The modeling of the corner crack at the nozzle-cylinder intersection

3.1.1. Location and orientation of the corner crack

The location of the corner crack at the nozzle-cylinder intersection is shown in Fig. 10(a). The orientation of the cracks, as shown in Fig. 10, is such that the cracks are perpendicular to the maximum principal stress which is the hoop stress [1]. In this orientation, the cracks are in mode-I (opening mode) in reference to the hoop stress which is the most detrimental stress for the RPV. For the definition of the corner crack, the crack tip position parameters: 'a, c, and ϕ' are also shown in Fig. 10(b).

The details of all the elliptical corner cracks postulated at the nozzle-cylinder intersection for the fracture analysis is given in Table 2.

3.1.2. The pallet body fracture model of the RPV

The 'pallet body fracture model' developed for the RPV having corner crack ($a = 0.25t$ and $a = 0.50c$) at nozzle-cylinder intersection is shown in Fig. 11(a). The close-up view of the finite element (FE) mesh around the crack front is shown in Fig. 11(b).

The hexahedral high quality mesh in the torus tube around the crack front is separately shown in Fig. 12. The mesh has been arranged in six layers of Soild-186 (20 nodes) elements. In order to capture the singular behaviour (stresses and strains) at the crack front, the first layer of the finite element (FE) mesh is modeled using 20 nodes collapsed quarter point singular elements. The details of the pallet body fracture model of the RPV in terms of number of elements, and number of nodes have been given in Ref. [1].

3.2. The fracture analysis under SB-LOCA conditions

Using the FE model of the crack RPV as shown in Fig. 11, the SIFs of the wide range of cracks under the SB-LOCA conditions are presented in this Section. The fracture evaluation and the determination of critical crack size under SB-LOCA conditions are also provided here.

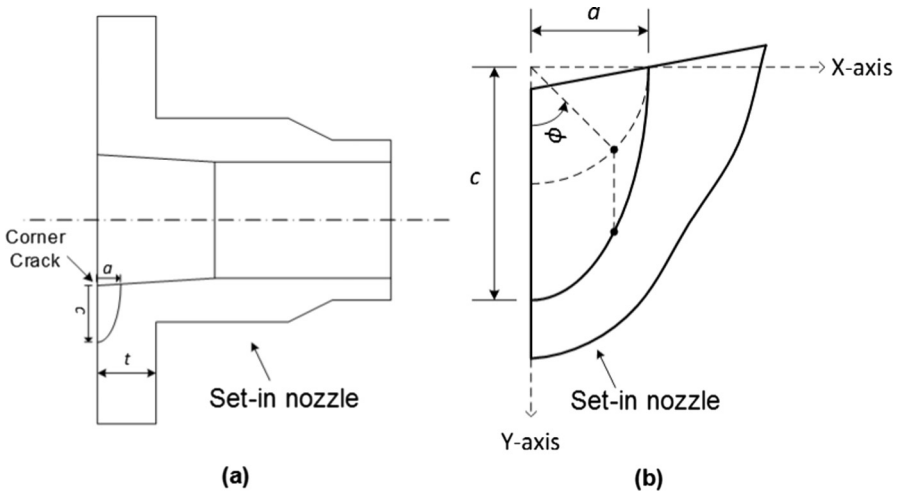

Fig. 10. The corner crack (a) location of the crack and (b) crack tip position parameters.

Table 2
Details of the corner cracks.

Corner cracks	Depth of corner crack	Elliptical corner cracks
1	$a/t = 0.01$	$a/c = 0.33$
2	$a/t = 0.05$	$a/c = 0.33$
3	$a/t = 0.10$	$a/c = 0.33$
4	$a/t = 0.15$	$a/c = 0.33$
5	$a/t = 0.20$	$a/c = 0.33$
6	$a/t = 0.25$	$a/c = 0.33$

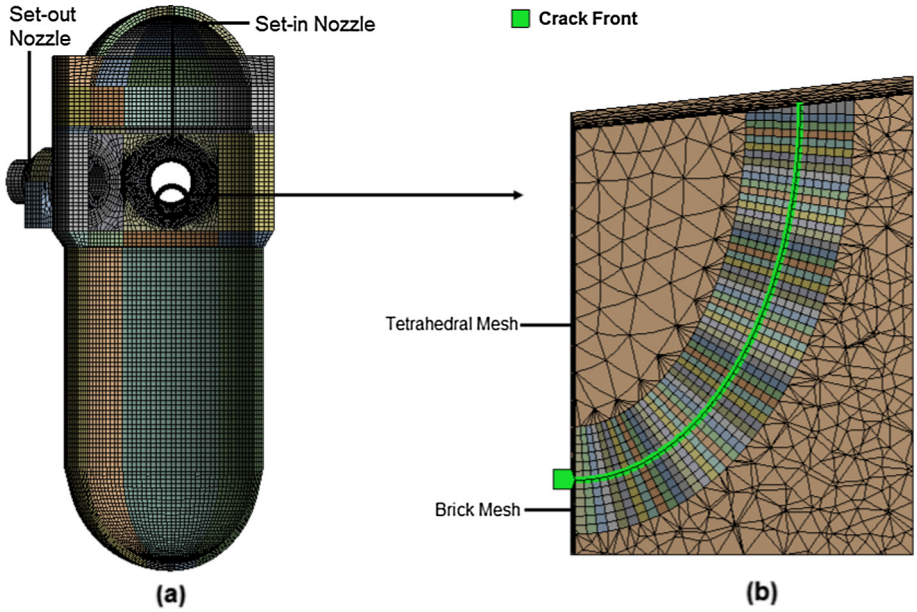

Fig. 11. The pallet body fracture model of the RPV (a) full view and (b) close-up view of the cracked region [1].

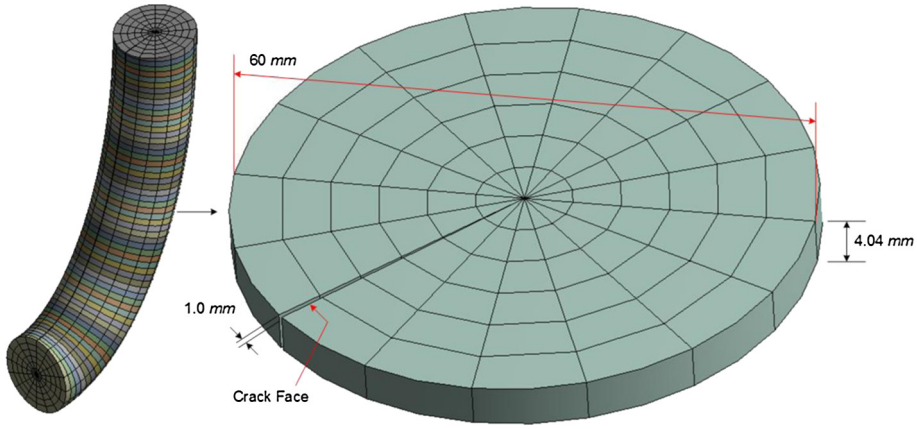

Fig. 12. Size of the elements around the crack front.

3.2.1. The LEFM based SIFs under SB-LOCA conditions

The 'LEFM based SIFs' of all the corner cracks (see Table 2) were computed at 0 sec, 1000 sec, 2000 sec, 3000 sec, 4000 sec, and 5000 sec of the SB-LOCA event. Fig. 13(a)–(f) present the SIFs (K_{IS}^{ps}) of the cracks having minor axis (a) equal to 1 percent, 5 percent, 10 percent, 15 percent, 20 percent, and 25 percent of the wall thickness (t), respectively. It is obvious from Fig. 13 (a)–(f) that for all types of the cracks, the 'maximum SIF' occurs at the specific time interval of 2000 sec where the drop rate in temperature (see Fig. 8) is the fastest during the SB-LOCA event. Hence, the PTS at 2000 sec is the most critical event during the SB-LOCA conditions. The SIF of the worst crack ($a = 0.25t$ and $a = 0.33c$), in this case, approaches $K_{IS,\max}^{ps} = 151.99\ \text{MPa}\sqrt{\text{m}}$ as shown in Fig. 13(f).

3.2.2. The EPFM based SIFs under SB-LOCA conditions

The 'EPFM based SIFs' of all the cracks under SB-LOCA conditions $\left(K_{JS}^{ps}\right)$ at 0 sec, 1000 sec, 2000 sec, 3000 sec, 4000 sec, and 5000 sec are presented in Fig. 14(a)–(f). Figures (a), (b), (c), (d), (e) and (f) show the SIFs of the cracks having minor axis (a) equal to 1 percent, 5 percent, 10 percent, 15 percent, 20 percent, and 25 percent of the wall thickness (t), respectively. The SIF of the worst crack ($a = 0.25t$ and $a = 0.33c$), in this case, approaches $K_{JS,\max}^{ps} = 142.65\ \text{MPa}\sqrt{\text{m}}$ as shown in Fig. 14(f).

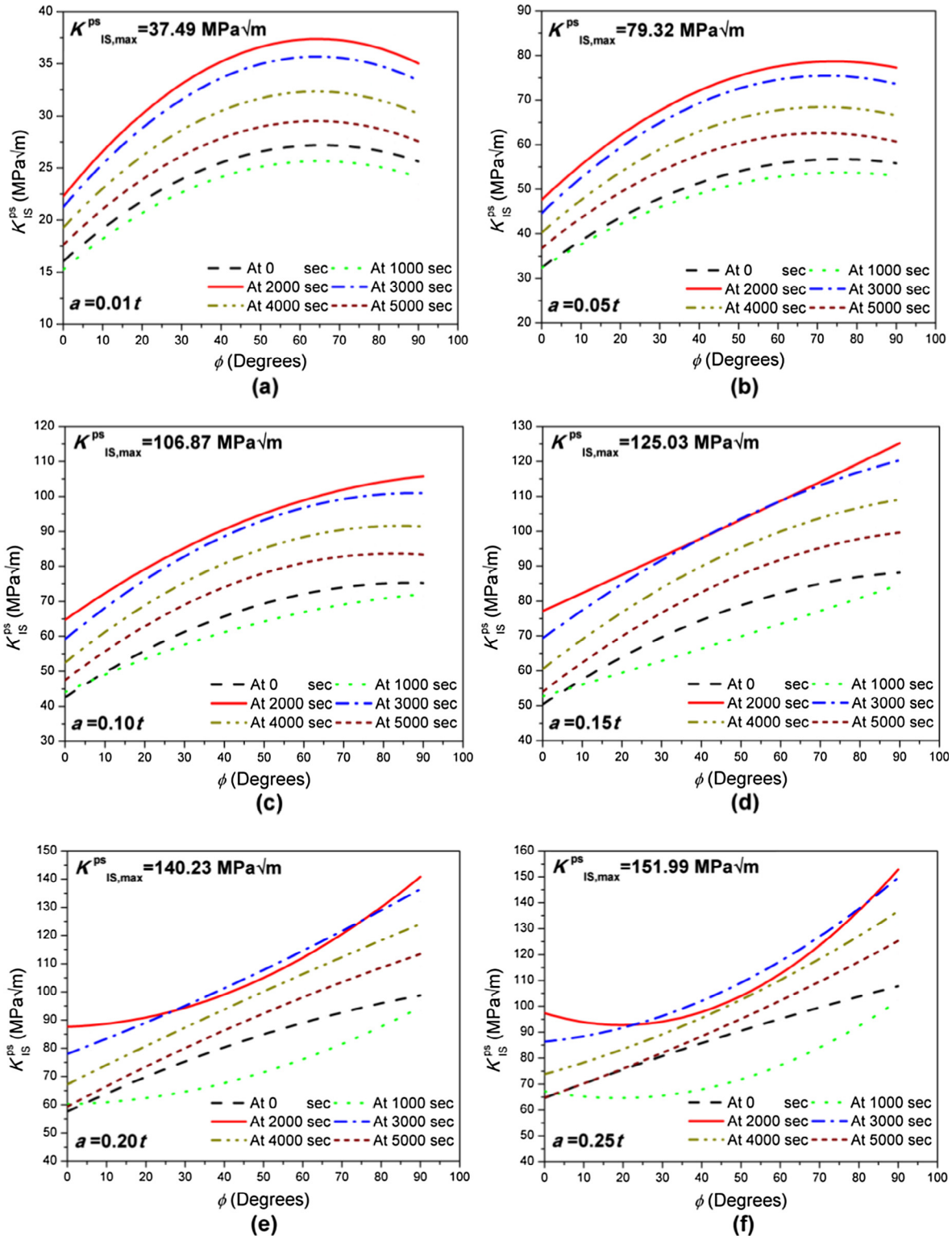

Fig. 13. The LEFM based SIFs under SB-LOCA conditions.

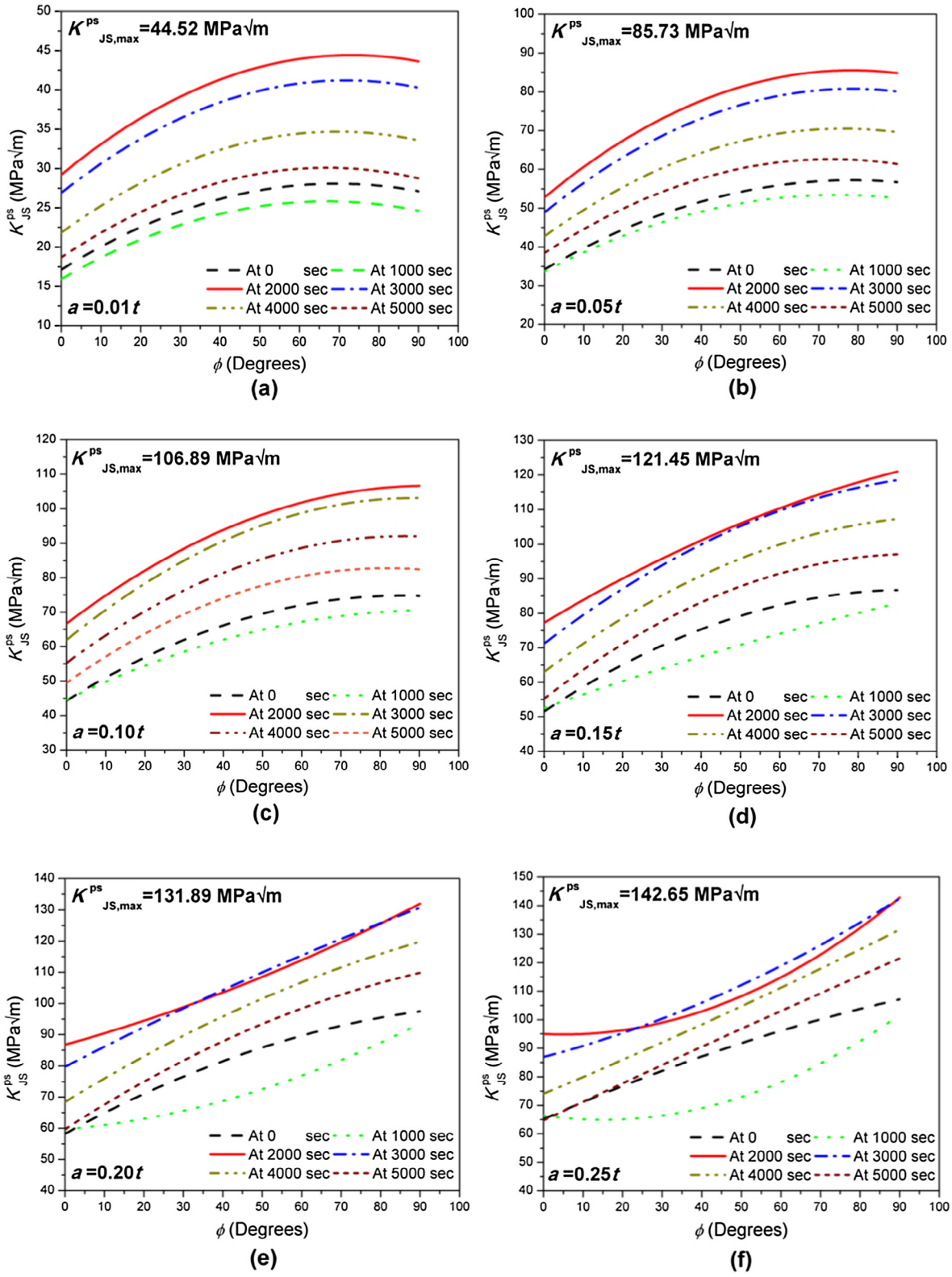

Fig. 14. The EPFM based SIFs under SB-LOCA conditions.

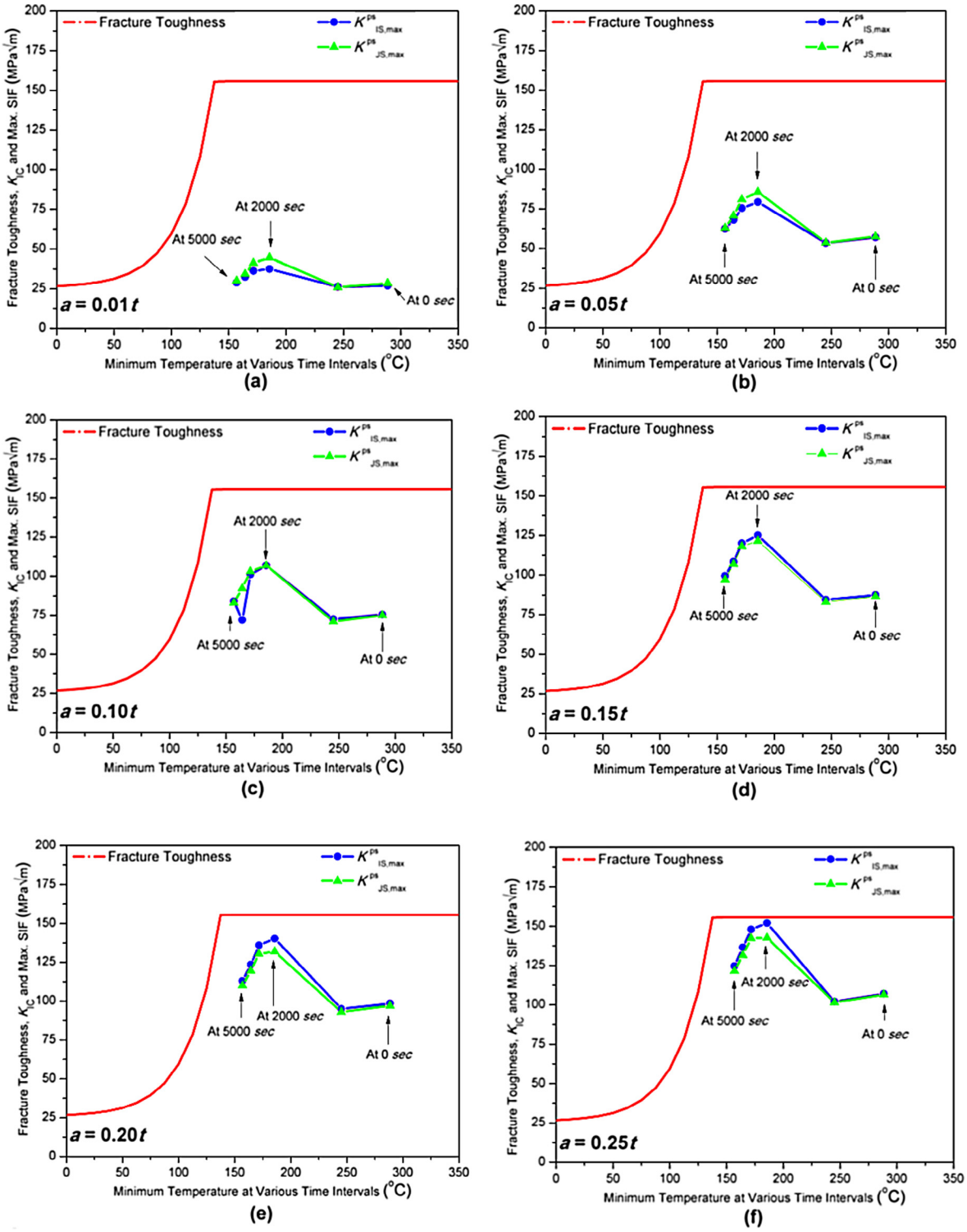

Fig. 15. The fracture evaluation under SB-LOCA conditions.

3.2.3. The fracture evaluation under SB-LOCA conditions

For the determination of critical crack depth under SB-LOCA conditions, the 'maximum SIFs' of all the corner cracks at time instant of 0 sec, 1000 sec, 2000 sec, 3000 sec, 4000 sec and 5000 sec, were compared with the fracture toughness of

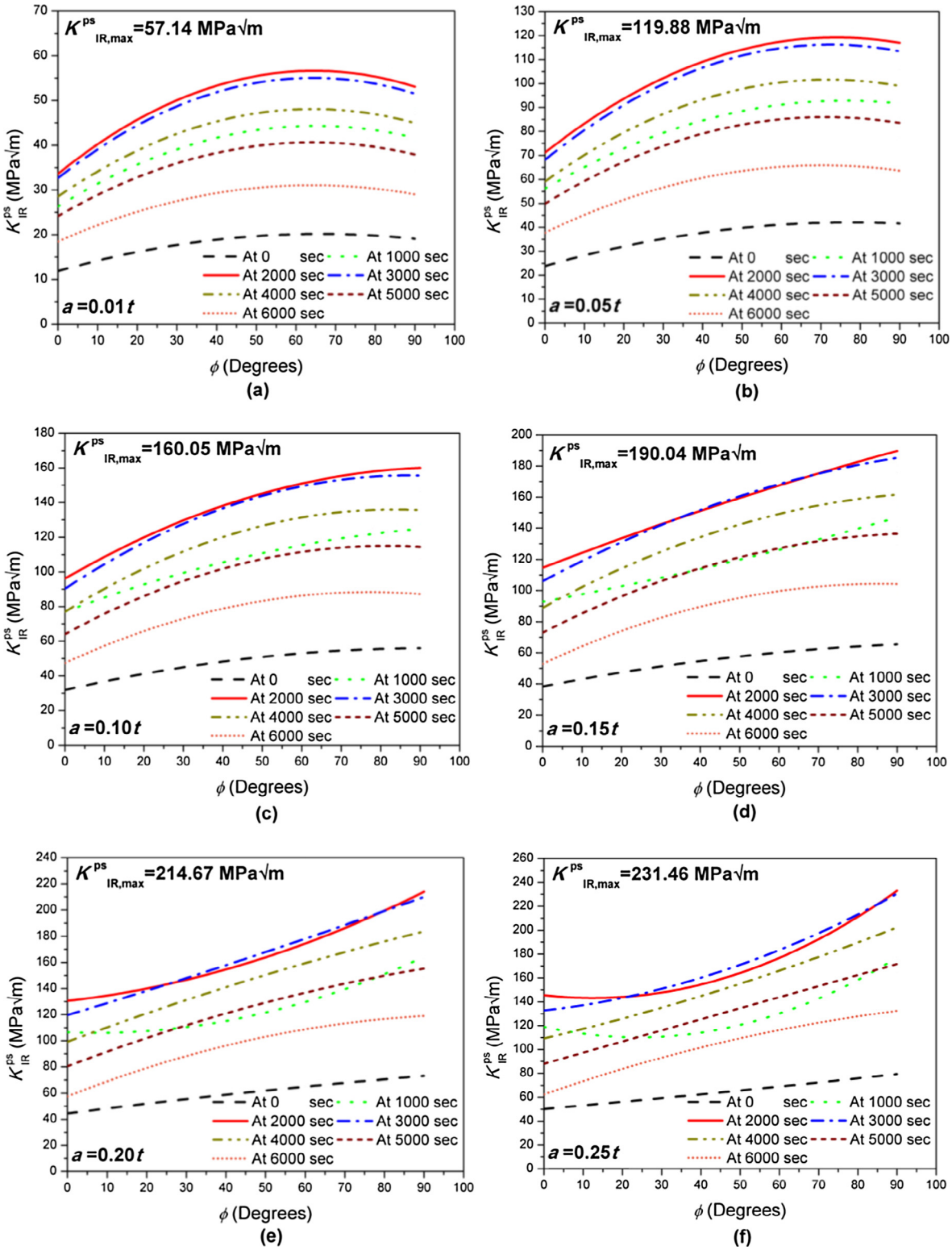

Fig. 16. The LEFM based SIFs under RST conditions.

the RPV's steel (see Fig. 5). The comparison has been presented in Fig. 15. Fig. 15(a)–(f) shows the comparison of the cracks having minor axis (a) equal to 1 percent, 5 percent, 10 percent, 15 percent, 20 percent, and 25 percent of the wall thickness (t), respectively.

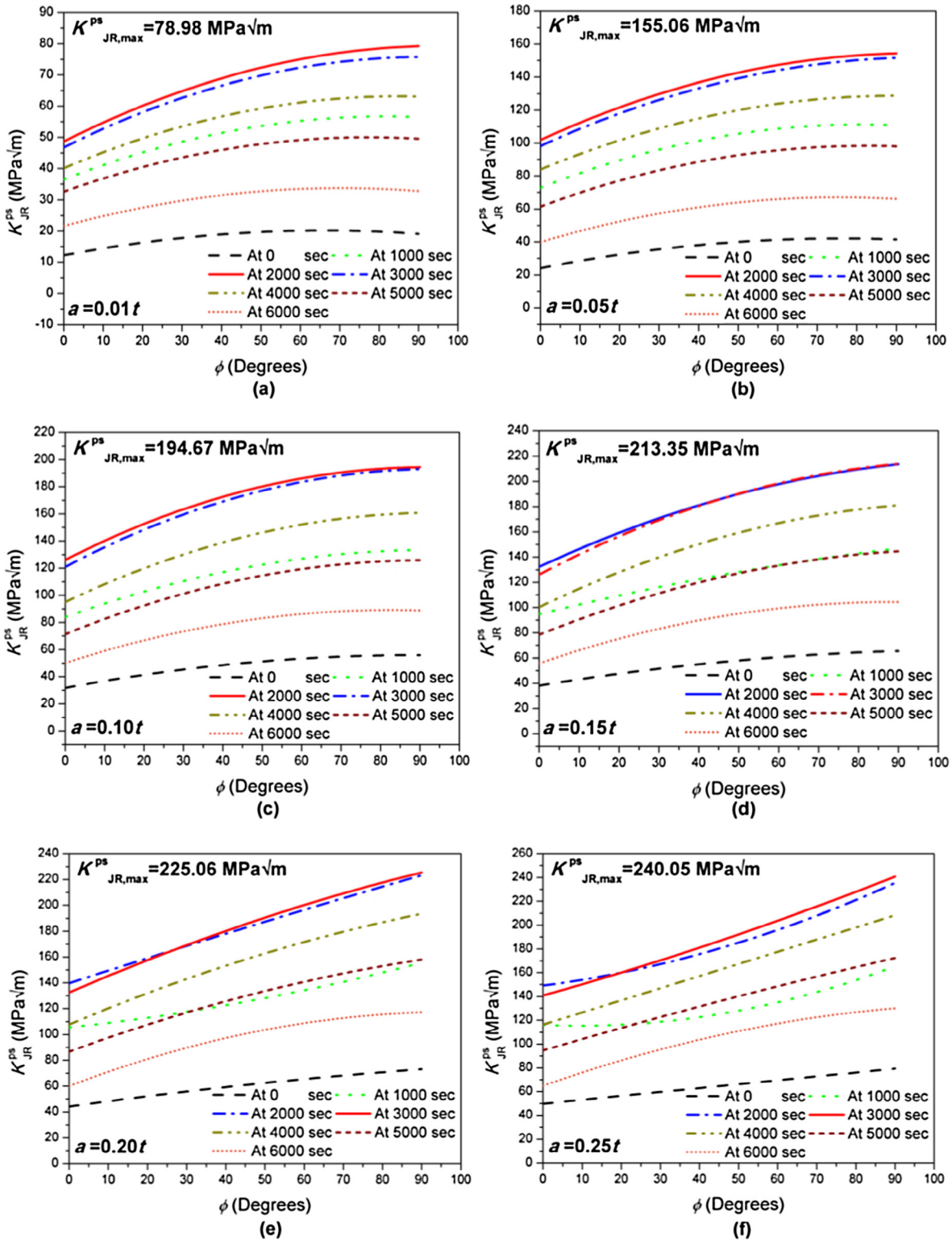

Fig. 17. The EPFM based SIFs under RST conditions.

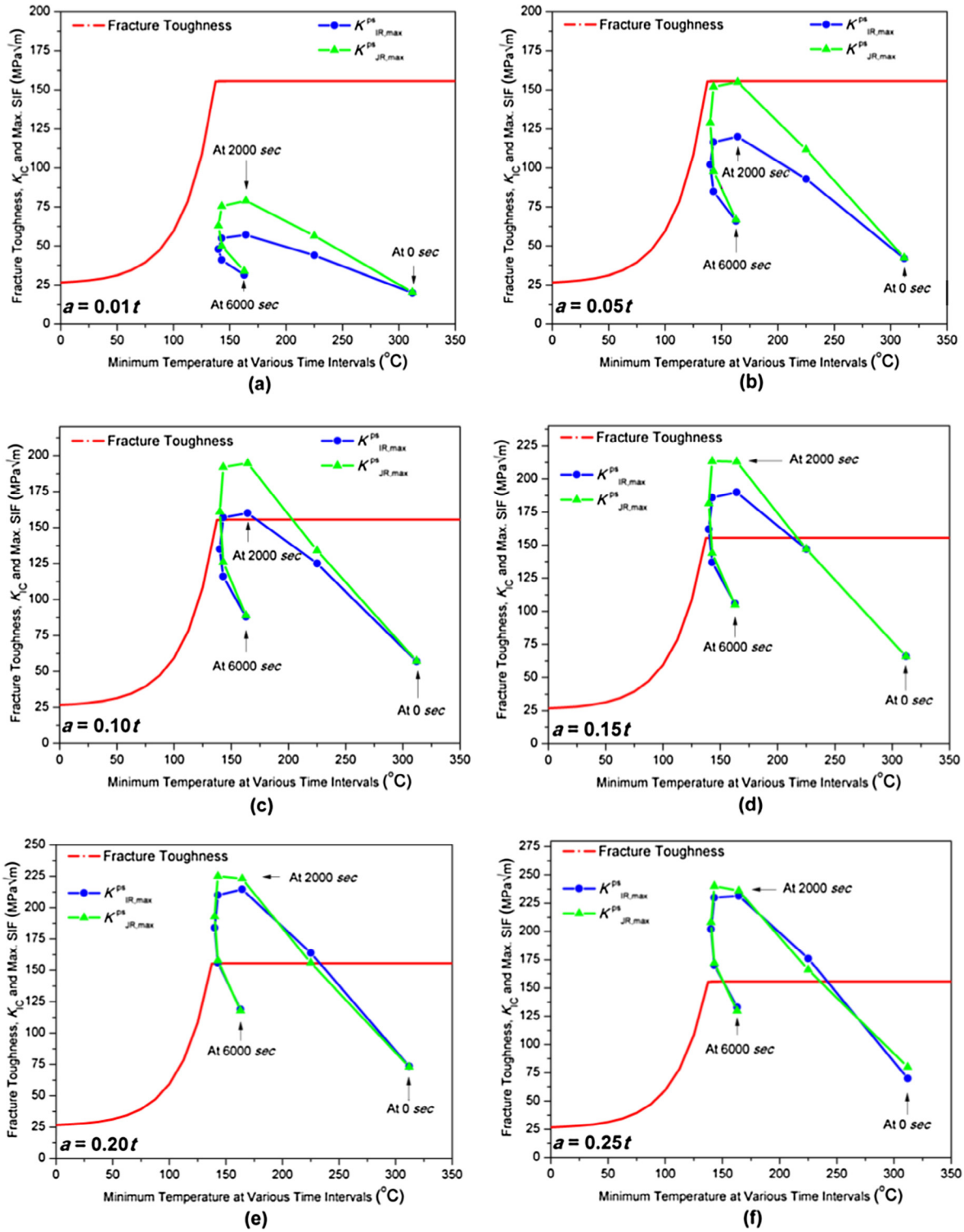

Fig. 18. The fracture evaluation under RST conditions.

It is evident from the results that all the corner cracks up to '$a = 0.25t$' have the SIFs which do not approach the fracture toughness of the material. Even the worst crack ($a = 0.25t$ and $a = 0.33c$) under the most severe event of SB-LOCA (at the time of 2000 sec) produces 'maximum SIF' equal to $K^{ps}_{JS,\max} = 151.99\ \text{MPa}\sqrt{\text{m}}$ which is below the fracture toughness value (see Fig. 15(f)).

3.3. The fracture mechanics analysis under RST conditions

The SIFs of all the corner cracks (see Table 2) under RST conditions are presented in this Section. The fracture evaluation and the determination of critical crack size under RST conditions are also provided.

3.3.1. The LEFM based SIFs under RST conditions

The 'LEFM based SIFs' under RST conditions (K_{IR}^{ps}) of all the corner cracks at the time instant of 0 sec, 1000 sec, 2000 sec, 3000 sec, 4000 sec, 5000 sec, and 6000 sec are presented in Fig. 16(a)–(f). Fig. 16(a)–(f) present the SIFs of the cracks having minor axis (a) equal to 1 percent, 5 percent, 10 percent, 15 percent, 20 percent, and 25 percent of the wall thickness (t), respectively. The 'LEFM based SIF' of the worst crack ($a = 0.25t$ and $a = 0.33c$), in this case, approaches $K_{IR,\max}^{ps} = 231.46\ \text{MPa}\sqrt{\text{m}}$ as shown in Fig. 16(f).

3.3.2. The EPFM based SIFs under RST conditions

The 'EPFM based SIFs' under RST conditions $\left(K_{JR}^{ps}\right)$ at 0 sec, 1000 sec, 2000 sec, 3000 sec, 4000 sec, 5000 sec, and 6000 sec have been presented in Fig. 17(a)–(f). Fig. 17(a)–(f) shows the SIFs of the cracks having minor axis (a) equal to 1 percent, 5 percent, 10 percent, 15 percent, 20 percent, and 25 percent of the wall thickness (t), respectively. The SIF of the worst crack ($a = 0.25t$ and $a = 0.33c$), in this case, approaches $K_{JR,\max}^{ps} = 240.05\ \text{MPa}\sqrt{\text{m}}$ as shown in Fig. 17(f).

3.3.3. The Fracture evaluation under RST conditions

Taking the 'maximum SIFs' of all the crack depths, at the time of 0 sec, 1000 sec, 2000 sec, 3000 sec, 4000 sec, 5000 sec, and 6000 sec, fracture evaluation under RST conditions in comparison to fracture toughness 'K_{IC}' has been presented in Fig. 18(a)–(f). It is obvious from Fig. 18(b) that the SIF of the crack having depth '$a = 0.05t = 20$ mm' is just approaching the fracture toughness value. Hence, the crack which is the 5 percent to the vessel's thickness ($a = 0.05t$) is the critical crack depth under RST conditions of the plant.

4. Conclusion

The fracture mechanics analysis of the set-in nozzle of a 300 MW reactor pressure vessel [4] has been performed under SB-LOCA and RST conditions of the pressurized water reactor. The SIFs for a wide range of corner surface cracks at the nozzle-cylinder intersection has been presented in a suitable graphical format, which provides a useful tool for the fracture analysis of the nozzle. The main conclusions drawn from the study can be summarized as follows:

- The RST conditions are more severe than the SB-LOCA conditions.
- Under SB-LOCA conditions; the SIFs of the corner cracks, up to depth '$a = 0.25t$', did not cross the fracture toughness value of the RPV's steel. Hence, the critical crack depth was not reached in this case.
- Under RST conditions; the SIF of the corner crack having depth '$a = 0.05t$' approaches the fracture toughness value. Hence, this crack has been finalized as the critical crack at the nozzle-cylinder intersection of the RPV.

Acknowledgements

The financial support of Pakistan Institute of Engineering and Applied Sciences (PIEAS) under IT & Telecom Endowment Fund is gratefully acknowledged.

References

[1] Murtaza UT, Hyder MJ. Stress intensity factors of corner cracks at set-in nozzle-cylinder intersection of a PWR reactor pressure vessel. J Braz Soc Mech Sci Eng 2016. http://dx.doi.org/10.1007/s40430-016-0522-x.
[2] Murtaza UT, Hyder MJ. Design by analysis versus design by formula of a PWR reactor pressure vessel. In: International multi conference of engineers and computer scientists.
[3] Murtaza UT, Hyder MJ. Optimization of the size and shape of the set-in nozzle for a PWR reactor pressure vessel. Nucl Eng Des 2015;284:219–27.
[4] Murtaza UT. Optimization and fracture mechanics analysis of the set-in nozzle of a PWR reactor pressure vessel [PhD Dissertation]. Islamabad: Pak. Inst. of Engg. and Appl. Sciences; 2016.
[5] ASME Boiler and Pressure Vessel Code, Section II, Part D: Properties, Materials; 2010.
[6] Murtaza UT, Hyder MJ. The effects of thermal stresses on the elliptical surface cracks in PWR reactor pressure vessel. Theor Appl Fract Mech 2015;75C:124–36.
[7] Murtaza UT, Hyder MJ. Methodology to analyze 3-D curved surface cracks using hybrid finite elements. In: International Young Engineers Convention.
[8] Murtaza UT, Hyder MJ. An approach for the assessment of semi elliptical surface crack. In: World Congress on Engineering.
[9] Bangash Y. PWR steel pressure vessel design and practice. Prog Nucl Energy 1985;16(1):1–40.
[10] Siegele D, Hodulak L, Varfolomeyev I, Nagel G. Failure assessment of RPV nozzle under loss of coolant accident. Nucl Eng Des 1999;193:265–72.
[11] Kim JS, Jin TE. Structural integrity assessment of the reactor pressure vessel under the external reactor vessel cooling condition. Nucl Eng Des 1999;191:117–33.
[12] He Y, Isozaki T. Fracture mechanics analysis and evaluation for the RPV of the Chinese Qinshan 300 MW NPP under PTS. Nucl Eng Des 2000;201:121–37.

[13] Çolak Ü, Özdere O. Comparative analysis of pressure vessel integrity for various LOCA conditions. J Nucl Mater 2001;297:271–8.
[14] Gülol OÖ, Çolak Ü. Comparison of pressure vessel integrity analyses and approaches for VVER 1000 and PWR vessels for PTS conditions. Nucl Eng Des 2003;226:231–41.
[15] Chen M, Lu F, Wang R, Ren A. Structural integrity assessment of the reactor pressure vessel under the pressurized thermal shock loading. Nucl Eng Des 2014;272:84–91.
[16] Guerrero MA, Betegon C, Belzunce J. Fracture analysis of a pressure vessel made of high strength steel (HSS). Eng Fail Anal 2008;15:208–19.
[17] Ramesh K. E-Book on engineering fracture mechanics. India: IIT Madras; 2007.
[18] Code of Federal Regulations. Fracture toughness requirements for protection against pressurized thermal shock events. Title 10, Part 50, Section 50.61 and Appendix G; 1996.
[19] USNRC Regulatory Guide 1.99. Rev. 2, Radiation embrittlement of reactor vessel materials; 1988.
[20] Kaplan I. Nuclear physics. 2nd ed. USA: Addison-Wesley Publishing Company; 1977.
[21] ASME Boiler and Pressure Vessel Code, Section III, Division 1, Appendix G: Fracture toughness criteria for protection against failure; 2010.
[22] ASME Boiler and Pressure Vessel Code, Section XI, Rules for in-service inspection of nuclear power plant components; 2010.
[23] API 579-1/ASME FFS-1 Fitness-For-Service standard. ANNEX F Material properties for A FFS assessment; 2007.
[24] Jhung MJ, Park YW. Deterministic fracture mechanics analysis of pressurized thermal shock. J Korean Nucl Soc 1998;30:470–84.
[25] Harvey JF. Theory and design of modern pressure vessels. 2nd ed. New York, USA: Van Nostrand Reinhold Company; 1974.
[26] U.S. Nuclear Regulatory Commission. Loss of integrated control system power and overcooling transient at Rancho Seco on December 26, 1985. USNRC Report NUREG 1195; 1986.